ρ = overall density $= \Sigma\rho_i$
ω_i = mass fraction of $i = \rho_i/\rho$
ω_{A1}, ω_{A2} = fixed mass fractions of A far from membrane (Figure 2)

Subscripts

A, B = species A, species B

Superscripts

I, III = bulk phase regions adjacent to membrane (Figure 2)
II = membrane region (Figure 2)

LITERATURE CITED

Anderson, B., and H. H. Ussing, "Solvent Drag on Non-Electrolytes During Osmotic Flow," *Acta Physiol. Scand.*, **39**, 228-239 (1957).

Bird, R. B., W. E. Stewart, and E. N. Lightfoot, *Transport Phenomena*, Wiley, New York (1960).

Froemter, E., G. Rumrich, and K. J. Ullrich, "Phenomenologic Description of Na^+, Cl^- and HCO_2 Absorption from Proximal Tubules of the Rat Kidney," *Pfluegers Arch. Eur. J. Physiol.*, **343**, 189-220 (1973).

Galey, W. R., and J. T. Van Bruggen, "The Coupling of Solute Fluxes in Membranes," *J. General Physiol.*, **55**, 220-242 (1970).

Ginzburg, B. Z., and A. Katchalsky, "The Frictional Coefficients of the Flow of Non-Electrolytes Through Artificial Membranes," *ibid.*, **47**, 403-418 (1963).

Hammond, B. R., and R. H. Stokes, "Diffusion in Binary Liquid Mixtures," *Trans. Faraday Soc.*, **49**, 890-895 (1953).

International Critical Tables, Vol. VII, p. 67, McGraw-Hill, New York (1930).

Kaufman, T. G., and E. F. Leonard, "Studies of Intramembrane Transport: A Phenomenological Approach," *AIChE J.*, **14**, 110-117 (1968).

Kedem, D., and A. Katchalsky, "Thermodynamic Analysis of the Permeability of Biological Membranes to Non-Electrolytes," *Biochimica et Biophysica Acta*, **27**, 229-246 (1958).

Kirkwood, J. G., "Transport of Ions Through Biological Membranes from the Standpoint of Irreversible Thermodynamics," in *Ion Transport Across Membranes*, H. T. Clarke and D. Nachmansohn, ed., Academic Press, New York (1954).

Lightfoot, E. N., Jr., *Transport Phenomena and Living Systems*, Wiley-Interscience, New York (1974).

Min, S., "Phenomenological Studies of Membrane Transport with a Wedge Interferometer," Ph.D. thesis, Pa. State Univ., University Park (1975).

———, J. L. Duda, and R. H. Notter, "Steady State Interferometric Studies of Membrane Transport," *Federation Proceedings Abstracts*, **34**, 325 (1975).

———, and J. S. Vrentas, "An Interferometric Technique for the Study of Steady State Membrane Transport," *AIChE J.*, **22**, 175-182 (1976).

Ochsenfahrt, H., and D. Winne, "The Contribution of Solvent Drag to the Intestinal Absorption of Tritiated Water and Urea from the Jejunum of the Rat," *Naunyn-Schmiedeberg's Arch. Pharmacol.*, **279**, 133-152 (1973).

———, "The Contribution of Solvent Drag to the Intestinal Absorption of the Basic Drugs Amidopyrine and Antipyrine from the Jejunum of the Rat," *ibid.*, **281**, 175-196 (1974*a*).

———, "The Contribution of Solvent Drag to the Intestinal Absorption of the Acidic Drugs Benzoic Acid and Salicylic Acid from the Jejunum of the Rat," *ibid.*, 197-217 (1974*b*).

Patlak. C. S., and S. I. Rapoport, "Theoretical Analysis of Net Tracer Flux Due to Volume Circulation in a Membrane with Pores of Different Sizes," *J. General Physiol.*, **57**, 113-124 (1971).

Perry, J. H., ed., *Chemical Engineering Handbook*, 3 ed., p. 188, McGraw-Hill, New York (1950).

Rosenberg, T., and W. Wilbrandt, "Uphill Transport Induced by Counterflow," *J. General Physiol.*, **41**, 289-296 (1957).

Ruch, T. E., and H. D. Patton, ed., *Physiology and Biophysics*, 19 ed., W. B. Saunders Co., Philadelphia, Pa. (1965).

Staverman, A. J., "Non-Equilibrium Thermodynamics of Membrane Processes," *Trans. Faraday Soc.*, **48**, 176-185 (1952).

Stender, S., K. Kristensen, and E. Skadhauge, "Solvent Drag by Solute-Linked Water Flow," *J. Membrane Biol.*, **11**, 377-398 (1973).

Tam, Y. M., "Characterization of Coupled Diffusion Effects with a Wedge Interferometer," M.S. thesis, Pa. State Univ., University Park (1976).

Ussing, H. H., "Some Aspects of the Application of Tracers in Permeability Studies," *Advances in Enzymology*, **13**, 21-65 (1952).

Manuscript received April 7, 1978; revision received October 30, and accepted January 11, 1979.

Fully Developed Viscous Flow and Heat Transfer in Curved Semicircular Sectors

The Navier-Stokes equation in stream function-vorticity form and the energy equation are solved numerically for a fully developed flow of a Newtonian fluid in coiled circular sectors having zero pitch. Two heat transfer cases are studied: axially uniform heat flux with uniform peripheral temperature and axially uniform temperature with mixed conditions along the periphery. Solutions are presented for curvature ratios in the range of 5 to 30, Prandtl numbers in the range of 0.7 to 100, and Dean numbers up to 300. In all cases studied, the heat transfer performance for the curved tubes was superior to that of a straight tube geometry.

JACOB H. MASLIYAH

Department of Chemical Engineering
University of Alberta
Edmonton, Alberta, Canada

and

K. NANDAKUMAR

Chemical Engineering Department
Princeton University
Princeton, New Jersey 08540

SCOPE

Curved tubes such as helical and spiral coils find a wide variety of application in heat exchangers and chemical reactors. The reason for such a wide use of coiled tubes are twofold. Coiled tubes make it possible to house process equipments such as heat exchangers in a very small space. More importantly, the existence of secondary flow in coiled tubes aids transfer processes such as convective heat and mass transfer.

Systematic study of transport phenomena in curved tubes started with the experimental work of Eustice (1910, 1911) and the theoretical work of Dean (1927). They studied the fluid flow in curved tubes of circular cross section. Recent contributions to this area include a rigorous numerical solution of the Navier-Stokes equation for a wide range of Dean numbers by Austin and Seader (1973). Kalb and Seader (1972, 1974) solved the energy equation under two different thermal boundary conditions. A review of all the work on pressure drop and heat transfer in coiled tubes of circular cross section can be found in Srinivasan et al. (1968). Curved tubes with noncircular cross section was first studied by Cuming (1952) who solved the equations of motion for flow through curved pipes of elliptical and square cross section. Other works on transport phenomena in curved tubes with different cross sections include Cheng and Akiyama (1970) who studied forced convective heat transfer in curved rectangular channels and Masliyah and Nandakumar (1977) who studied forced convective heat transfer in internally finned helical coils.

The main objective of the present study is to obtain numerical solutions for the fully developed fluid flow and heat transfer with two different thermal boundary conditions. The configuration under study is coiled tubes with a cross section of circular sectors as shown in Figure 1*a*. Analytical study of fluid flow and heat transfer in straight tubes with a cross section of circular sectors can be found in Eckert et al. (1958).

CONCLUSIONS AND SIGNIFICANCE

A numerical study of fully developed viscous flow and heat transfer for two different thermal boundary conditions in curved semicircular sectors has been presented. A computer program developed to solve the governing equations is quite general and is capable of handling any curved circular sector geometry shown in Figure 1*c*. However, the results are presented only for semicircular sectors shown in Figure 1*a*.

The friction factors can be adequately correlated by Dean number alone, and they do not depend on the radius of curvature as an additional parameter. For the two cases of thermal boundary conditions, the average Nusselt number depends on both Dean number and Prandtl number. A comparison of results with fluid flow and heat transfer in curved rectangular tubes indicates that the equivalent diameter is not adequate to account for the two different geometries.

The fractional increase in heat or mass transfer coefficient relative to the fractional increase in friction factor for curved and straight semicircular ducts is greater than unity for all cases studied, and it increases with both Dean and Prandtl numbers.

Such a heat transfer enhancement is for the case of helical coils of very small pitch. For cases of loosely wound coils, it is likely that the enhancement in heat transfer becomes lower than the ideal case considered here.

Curved tubes such as helical and spiral coils are known to enhance the transfer processes such as heat and mass transfer. This is due to the existence of secondary flow field which is superimposed upon the axial velocity flow field. Fundamental information on the velocity field is useful in establishing heat and mass transfer rates and homogeneous chemical kinetic phenomena for flow in curved tubes. Recently, interest has been expressed in increasing mass transfer rates in membrane blood oxygenators, (Weissman and Mockros, 1968) by making use of secondary flows such as those induced by curved tube flow channels. For these reasons, the transport phenomena in curved tubes of various cross sections have received much attention in the literature. Kalb and Seader (1972) have shown that the fractional increase in heat transfer coefficients relative to the fractional increase in friction factors for curved circular tubes as compared to circular straight tubes could be as high as 2.5. Similar behavior was predicted for rectangular curved tubes by Cheng and Akiyama (1970) and Cheng and Hwang (1969). Transition from laminar to turbulent flow is much delayed in helical tubes. Taylor's (1929) experiments showed that depending on the ratio of radius of curvature to tube radius, the critical Reynolds number was increased to values beyond the value of 2 100 usually accepted for straight tubes. For example, for a curvature ratio of 18.7, a critical Reynolds number of 5 830 was observed. Such results for critical Reynolds number are not available at present for curved tubes with noncircular cross sections.

Several theoretical studies by Dean (1927), Topakoglu (1967), McConalogue and Srivastava (1968), Truesdell and Adler (1970), Akiyama and Cheng (1971), and Austin and Seader (1973) are available on flow in curved tubes of a circular cross section. Theoretical studies on transport phenomena in curved tubes with a noncircular cross section are given by Cuming (1952) and Cheng and Hwang (1969).

Here we present a detailed numerical solution for fluid flow and heat transfer in curved semicircular ducts as shown in Figure 1*a*. Such tubes can be used as heat exchangers wound around cylindrical vessels with the flat surface of the coil contacting the cylindrical surface as shown in Figure 1*b*. The equations of motion and energy are solved in toroidal coordinate system. While the results presented in this work are for a configuration such as that of Figure 1*a*, the developed computer program is more general and is capable of solving a case such as that of Figure 1*c*.

Solutions for heat transfer are presented for two different thermal boundary conditions.

Case 1. Uniform axial heat flux with uniform peripheral temperature.

Case 2. Uniform axial temperature with peripheral conditions of uniform temperature along the straight inner wall and zero heat flux for the outer semicircular surface. Such a condition will be useful for the case shown in Figure 1*b*.

GOVERNING EQUATIONS

The equations of motion for the case of a fully developed, incompressible viscous flow of a Newtonian fluid with constant physical properties in toroidal coordinate system are given below. The variables are rendered

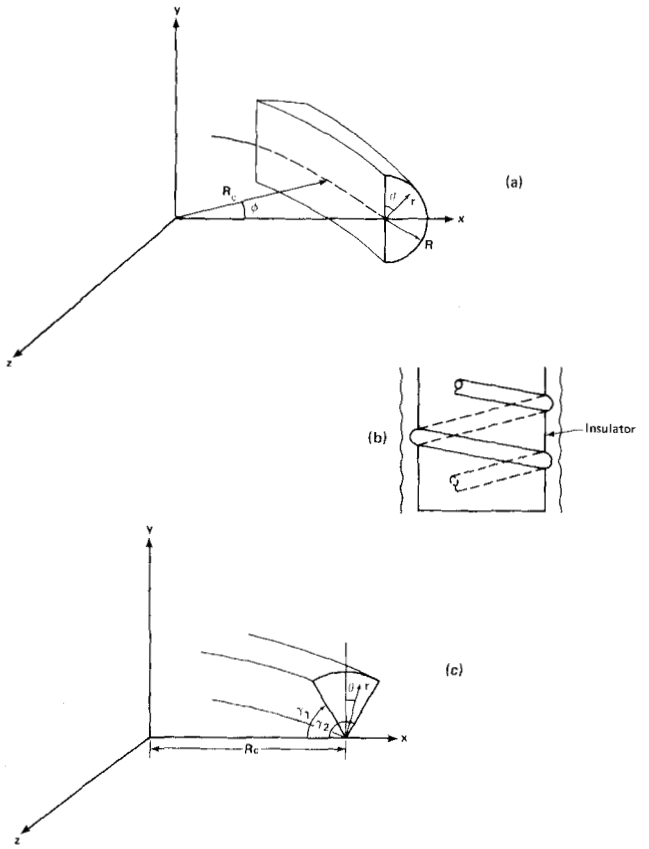

Fig. 1. Geometry of helical semicircular sectors.

dimensionless using the following quantities:

$$r = \frac{r'}{R} \quad \lambda = \frac{Rc}{R} \quad v_r = \frac{v'_r}{(\nu/R)} \quad v_\theta = \frac{v'_\theta}{(\nu/R)}$$

$$Q = \frac{\partial p'}{\partial \phi}\frac{R^2}{\nu\mu} \quad v_\phi = \frac{v'_\phi}{(\nu/R)} \quad \omega_\phi = \frac{\omega'_\phi}{(\nu/R^2)}$$

and

$$\psi = \psi'/\nu R$$

1. Axial component of Navier-Stokes equation:

$$A_v v_\phi + B\frac{\partial v_\phi}{\partial \theta} + C\frac{\partial v_\phi}{\partial r} - \frac{\partial^2 v_\phi}{\partial r^2} - \frac{1}{r^2}\frac{\partial^2 v_\phi}{\partial \theta^2} = -\frac{Q}{H} \tag{1}$$

where

$$A_v = \frac{1}{H^2}\left[1 - \left(\frac{\sin\theta}{r}\right)\frac{\partial \psi}{\partial \theta} + \cos\theta\frac{\partial \psi}{\partial r}\right]$$

$$B = \frac{1}{rH}\left[\frac{\partial \psi}{\partial r} - \cos\theta\right]$$

$$C = -\left[\frac{1}{r} + \frac{\sin\theta}{H} + \frac{1}{rH}\frac{\partial \psi}{\partial \theta}\right]$$

$$H = \lambda + r\sin\theta$$

2. Vorticity transport equation:

$$A_\omega \omega_\phi + B\frac{\partial \omega_\phi}{\partial \theta} + C\frac{\partial \omega_\phi}{\partial r} - \frac{\partial^2 \omega_\phi}{\partial r^2} - \frac{1}{r^2}\frac{\partial^2 \omega_\phi}{\partial \theta^2} = D \tag{2}$$

where

$$A_\omega = \frac{1}{H^2}\left[1 - \cos\theta\frac{\partial \psi}{\partial r} + \frac{\sin\theta}{r}\frac{\partial \psi}{\partial \theta}\right]$$

$$D = \frac{2v_\phi}{H}\left[\cos\theta\frac{\partial v_\phi}{\partial r} - \frac{\sin\theta}{r}\frac{\partial v_\phi}{\partial \theta}\right]$$

3. Stream function-vorticity equation:

$$\frac{1}{H}\frac{\partial^2 \psi}{\partial r^2} + \frac{1}{Hr^2}\frac{\partial^2 \psi}{\partial \theta^2} + \frac{\lambda}{rH^2}\frac{\partial \psi}{\partial r} - \frac{\cos\theta}{rH^2}\frac{\partial \psi}{\partial \theta} = \omega_\phi \tag{3}$$

The defining equations of stream function are

$$v_r = \frac{-1}{r(\lambda + r\sin\theta)}\frac{\partial \psi}{\partial \theta} \tag{4}$$

$$v_\theta = \frac{1}{(\lambda + r\sin\theta)}\frac{\partial \psi}{\partial r} \tag{5}$$

The axial vorticity is given by

$$\omega_\phi = \frac{\partial v_\theta}{\partial r} + \frac{v_\theta}{r} - \frac{1}{r}\frac{\partial v_r}{\partial \theta} \tag{6}$$

Subject to the no-slip boundary condition at the surface, Equations (1) to (3) describe the flow field in a curved semicircular sector. Owing to the manner in which the variables are rendered dimensionless, the pressure drop appears explicitly in the equation for axial velocity, and the Reynolds number becomes an implicit quantity to be calculated from the velocity field.

BOUNDARY CONDITIONS

The three dependent variables, namely, the axial velocity v_ϕ, the stream function ψ, and the vorticity ω_ϕ, are to be specified on the flow boundary:

$v_\phi = 0$	$r = 1$	$0 \le \theta \le \frac{\pi}{2}$	(no slip)
$v_\phi = 0$	$r = 0$	$0 \le \theta \le \frac{\pi}{2}$	
$v_\phi = 0$	$0 \le r \le 1$	$\theta = 0$	(no slip)
$\frac{\partial v_\phi}{\partial \theta} = 0$	$0 \le r \le 1$	$\theta = \frac{\pi}{2}$	(symmetry)
$\psi = 0$	$r = 1$	$0 \le \theta \le \frac{\pi}{2}$	
$\psi = 0$	$0 \le r \le 1$	$\theta = 0$	
$\psi = 0$	$0 \le r \le 1$	$\theta = \frac{\pi}{2}$	(symmetry)
$\psi = 0$	$r = 0$	$0 \le \theta \le \frac{\pi}{2}$	
$\omega_\phi = \frac{\partial v_\theta}{\partial r} = \frac{1}{H}\frac{\partial^2 \psi}{\partial r^2}$	$r = 1$	$0 \le \theta \le \frac{\pi}{2}$	
$\omega_\phi = 0$	$r = 0$	$0 \le \theta \le \frac{\pi}{2}$	
$\omega_\phi = \frac{1}{Hr^2}\frac{\partial^2 \psi}{\partial \theta^2}$	$0 < r < 1$	$\theta = 0$	
$\omega_\phi = 0$	$0 < r < 1$	$\theta = \frac{\pi}{2}$	(symmetry)

The Reynolds number $D'e\ \rho\ \overline{v'}_\phi/\mu$ based on the equivalent diameter is given by

$$Re = De\,\overline{v}_\phi \tag{7}$$

$$De = \frac{4V'_w}{RA'_w} = 4V_w/A_w \tag{8}$$

where

$$De = D'e/R,\ V_w = V'_w/R^3 \text{ and } A_w = A'_w/R^2$$

V'_w and A'_w are the wetted volume and the wetted area per unit ϕ, respectively. This less common, but more general, definition of the equivalent diameter is preferred because in this particular geometry the tube is not symmetric about $\theta = 0$. To reflect the nature of the asymmetry, which is caused by the curvature of the tube, the definition given by Equation (8) is used for the equivalent diameter. This results in the following expression for the equivalent diameter:

$$De = \frac{4\left[\frac{\lambda\pi}{2} + \frac{2}{3}\right]}{\lambda(\pi + 2) + 2} \tag{9}$$

As $\lambda \to \infty$, $De \to 2\pi/(\pi + 2)$, which is the value of the equivalent diameter for a straight semicircular sector. The product fRe for the curved semicircular sector is given by

$$fRe = \left(\frac{2Q}{\bar{v}_\phi}\right)(A_x De/A_w) \tag{10}$$

Equation (10) was arrived at using the definition of friction factor, where

$$-(\Delta p')A'_x = \tfrac{1}{2}\,\bar{\rho}\bar{v}'^2_\phi A'_w(\Delta\phi)f \tag{11}$$

and

$$A_x = A'_x/R^2$$

The validity of the numerical solution can be checked by integrating the wall shear stress $\tau'_{r\phi}$ and $\tau'_{\theta\phi}$ and equating the total shear force to the pressure force. This force balance leads to

$$2\int_0^1 \lambda\tau_{\theta\phi}dr + \int_0^\pi \tau_{r\phi}(\lambda + r\sin\theta)d\theta = \frac{\pi Q}{2} \tag{12}$$

where the dimensionless shear stress at a respective surface is given by

$$\tau_{\theta\phi} = \frac{1}{r}\frac{\partial v_\phi}{\partial\theta} \tag{13}$$

and

$$\tau_{r\phi} = \frac{\partial v_\phi}{\partial r} \tag{14}$$

The shear stress is rendered dimensionless using

$$\tau' = \mu^2\tau/R^2\rho$$

HEAT TRANSFER

The steady state energy equation for constant fluid properties, negligible energy dissipation, and negligible axial conduction is given by

$$v'_r\frac{\partial T'}{\partial r'} + \frac{v'_\theta}{r}\frac{\partial T'}{\partial\theta} + \frac{v'_\phi}{(Rc + r'\sin\theta)}\frac{\partial T'}{\partial\phi} = \frac{\nu}{Pr}\left[\frac{\partial^2 T'}{\partial r'^2} + \frac{1}{r'}\frac{\partial T'}{\partial r'} + \frac{\sin\theta}{(Rc + r'\sin\theta)}\frac{\partial T'}{\partial r'} + \frac{1}{r'^2}\frac{\partial^2 T'}{\partial\theta^2} + \frac{\cos\theta}{r'(Rc + r'\sin\theta)}\frac{\partial T'}{\partial\theta}\right] \tag{15}$$

For any particular boundary condition, Rohsenow and Choi (1961), a fully developed temperature profile is assumed to exist when

$$\frac{T'_w - T'}{T'_w - T'_b} = f(r', \theta) \tag{16}$$

For axially uniform wall heat flux condition with peripherally uniform temperature (case 1), Equation (16) leads to

$$\frac{dT'_w}{d\phi} = \frac{\partial T'}{\partial\phi} = \frac{dT'_b}{d\phi} \tag{17}$$

For the case of axial uniform temperature with peripheral conditions of uniform wall temperature, T'_w, at the flat tube section and adiabatic surface for the semicircular tube section (case 2), Equation (16) leads to

$$\frac{\partial T'}{\partial\phi} = \frac{dT'_b}{d\phi}f(r', \theta) = \frac{T'_w - T'}{T'_w - T'_b}\frac{dT'_b}{d\phi} \tag{18}$$

Equations (17) and (18) are then used in (15) to replace $\partial T'/\partial\phi$. If we define a dimensionless temperature T as

$$T = \frac{(T'_w - T')\lambda}{RePr(dT'_b/d\phi)} \tag{19}$$

the energy Equation (15) becomes

$$\frac{\partial^2 T}{\partial r^2} + \frac{1}{r^2}\frac{\partial^2 T}{\partial\theta^2} + \left[\frac{1}{r} + \sin\theta/(\lambda + r\sin\theta) - v_r Pr\right]\frac{\partial T}{\partial r} + \left[\frac{\cos\theta}{r(\lambda + r\sin\theta)} - \frac{v_\theta Pr}{r}\right]\frac{\partial T}{\partial\theta} + A = 0 \tag{20}$$

where, for case 1

$$A = \frac{v_\phi\lambda}{Re(\lambda + r\sin\theta)} \tag{21}$$

and for case 2

$$A = \frac{v_\phi\lambda T}{T_b Re(\lambda + r\sin\theta)} \tag{22}$$

The appropriate boundary conditions for the energy equation are

	$T = 0$	$0 \le r \le 1$	$\theta = 0$
	$\frac{\partial T}{\partial\theta} = 0$	$0 \le r \le 1$	$\theta = \pi/2$
case 1	$T = 0$	$r = 1$	$0 \le \theta \le \pi/2$
case 2	$\frac{\partial T}{\partial r} = 0$	$r = 1$	$0 \le \theta \le \pi/2$

The dimensionless bulk fluid temperature T_b is given by

$$T_b = \frac{\int_0^\pi\int_0^1 v_\phi T r dr d\theta}{\bar{v}_\phi A_x} \tag{23}$$

The average heat transfer coefficient $\bar{h}$ is given by

$$\bar{q} = \bar{h}(T'_w - T'_b) \tag{24a}$$

An energy balance gives

$$\frac{\bar{q}A'_h}{\bar{v}'_\phi A'_{x\rho}Cp} = \frac{\Delta T'_b}{\Delta\phi} \tag{24b}$$

Using Equations (19) and (24), one obtains

$$\bar{Nu} = \frac{\bar{h}D'e}{k} = \frac{\lambda A_x}{T_b A_h} \tag{25}$$

where

$$A_h = A'_h/R^2$$

For case 1, $A_h = A_w$, and for case 2, $A_h = 2\lambda$. The local heat transfer coefficient is given by

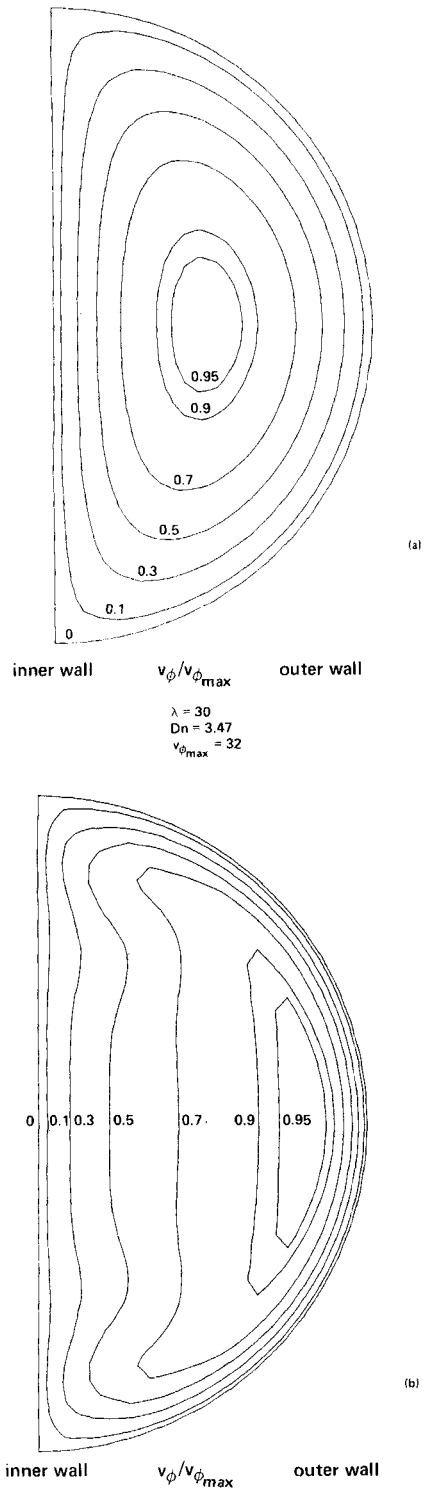

Fig. 2. Contours of normalized dimensionless axial velocity for λ = 30.

$$h(T'_w - T'_b) = -k\frac{\partial T'}{\partial n}\bigg|_{\text{surface}} \tag{26}$$

The above equation leads to

$$Nu(\theta) = \frac{hD'e}{k} = -\frac{De}{T_b}\frac{\partial T}{\partial r}\bigg|_{r=1}$$

at the semicircular tube section, and

$$Nu(r) = \frac{De}{T_b r}\frac{\partial T}{\partial \theta}\bigg|_{\theta=0}$$

at the straight section. The average Nusselt number can also be expressed in terms of the local Nusselt number by

$$\overline{Nu} = \frac{1}{A_h}\left[2\int_0^1 \lambda Nu(r)\,dr + \int_0^\pi [\lambda + \sin\theta]Nu(\theta)\,d\theta\right] \tag{27}$$

Obviously, for case 2, the second integral is zero.

METHOD AND VALIDITY OF SOLUTION

The fluid flow and the energy equations were solved using a second-order central difference approximation. A relaxation method was used in conjunction with the modified scheme of calculation as presented by Wilkes (1966), whereby two subgrids were used for each of the flow parameters. This approach was found to be at least twice as fast as that of the traditional SOR method. The computational details are given elsewhere (Masliyah and Nandakumar, 1977). Convergence of the results was assumed when the relative error tolerance, defined as

$$E = \left|\frac{G_{n+1} - G_n}{G_{n+1}}\right|$$

was less than 10^{-4}, where n refers to the n^{th} iteration. Apparent convergence in the values of $f\,Re$ (or $\overline{v_\phi}$) and $\overline{Nu}$ (or T_b) was found to be a poor indication for the convergence of the local flow parameter, as both $f\,Re$ and $\overline{Nu}$ were obtained from an averaging procedure. Using a grid size of $\Delta r = 0.05$ and $\Delta\theta = \pi/30$, for $\lambda = 1\,000$ (a straight semicircular sector), $f\,Re$ was given as 15.79. The accepted value is 15.77 (Shah and London, 1971). The corresponding average Nusselt number for case 1 was found to be 4.078. The literature value is 4.088 (Sparrow and Haji-Skeikh, 1965). For case 2, the average Nusselt number was 2.816. No literature value for $\overline{Nu}$ for this heat transfer case is available. However, the computed $\overline{Nu}$ value lies between two limiting cases for a rectangle of an aspect ratio of 2, with one surface and three surfaces being adiabatic; the respective Nusselt numbers are 2.602 and 3.185 (Shah and London, 1971).

A grid size of $\Delta r = 5/100$ and $\Delta\theta = \pi/30$ was used in this study for cases of a Dean number less than 150. For $Dn > 150$, the grid size was reduced to $\Delta r = 3/100$ and $\Delta\theta = \pi/60$. Using the smaller grid size, the values of $f\,Re$ did not change by more than 0.5%. However, the agreement between the left-hand side of Equation (12) and its right-hand side was much improved using the smaller grid size. In most cases, the agreement between both sides of Equation (12) was within 2%. This type of comparison as provided by Equation (12) is essential in checking the validity of the numerical solution.

Values for the average Nusselt number as evaluated by Equations (25) and (27) varied as much as 20% for the coarse grid. The disagreement was larger for the case of high Prandtl and Dean numbers. However, for $Pr = 0.7$ and $Dn < 20$, the values of $\overline{Nu}$ as obtained by the two equations were in fair agreement. On decreasing the grid size, little change (less than 1%) in the value of $\overline{Nu}$ as given by Equation (25) was observed. However, the $\overline{Nu}$ value as given by Equation (27) was very much affected (a change of about 10%) by the grid size reduction. Close examination of the temperature

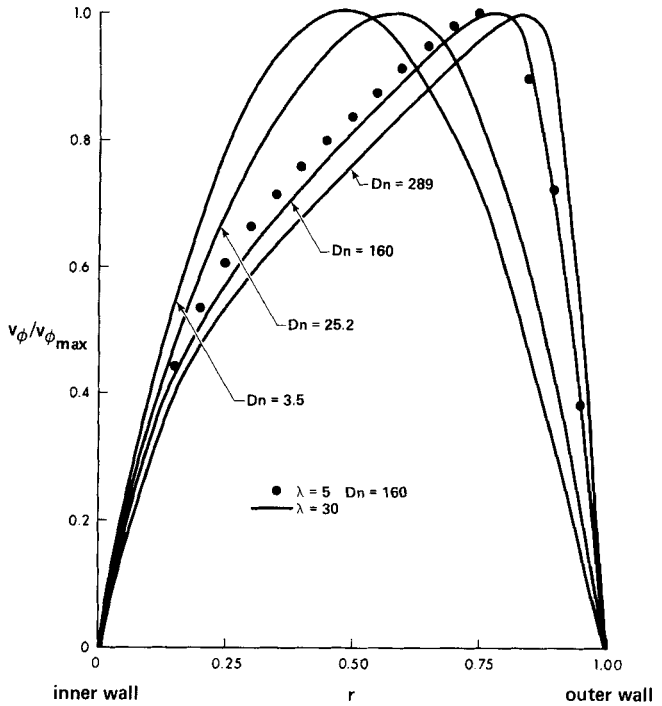

Fig. 3. Radial variation of normalized dimensionless axial velocity for $\lambda = 30$ (and 5) at $\theta = \pi/2$.

profile along $\theta = 0$ for $0 \leq r \leq 1$ indicates that as Pr and Dn are increased, the temperature gradient at the wall becomes very steep, and consequently differentiation at the wall region gives rise to fairly large errors. These errors are manifested in the values of $\overline{Nu}$ as given by Equation (27). When Dn and Pr are small, the temperature gradient at the wall is not steep, and consequently good agreement for $\overline{Nu}$ as given by Equations (25) and (27) are expected.

The reported $\overline{Nu}$ values were evaluated using Equation (25).

DISCUSSION OF RESULTS

Fluid Flow

Contours of normalized axial velocity profile are shown in Figures 2*a* and 2*b* for $Dn = 3.47$ and 289, respectively. For the higher Dean number case, the axial velocity away from the tube walls becomes fairly constant for a given vertical surface of a radius less than about $\lambda + 3/4$. The profile is essentially linear near the central part of the flow field with steep gradients close to the walls corresponding to a boundary layer. This observation is useful in confirming the applicability of the boundary layer approximation at the high Dean number limit. Such an approach has been used previously by Mori and Uchida (1967). The above-mentioned behavior is brought out more clearly in Figure 3, where normalized axial velocity is given as a function of position along $\theta = \pi/2$. From both Figures 2 and 3, it is observed that as Dn number increases, which may be due to an increase in Re or a decrease in radius of curvature, the maximum axial velocity occurs closer to the outer wall, and this shift occurs along the $\theta = \pi/2$ line. This is similar to the case of flow in curved circular tubes (Austin and Seader, 1973) but differs from the prediction of Joseph et al. (1975) who observed that for flow in curved square tubes beyond a certain Dean number (about 200), the location of the maximum axial velocity moves away

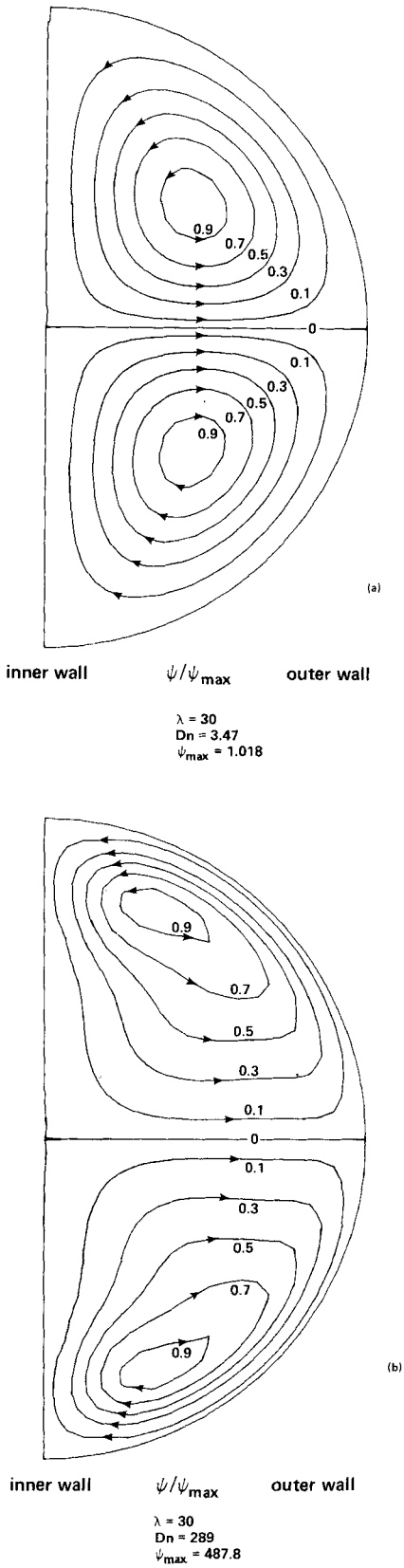

Fig. 4. Contours of normalized dimensionless secondary stream function for $\lambda = 30$.

from the horizontal line of symmetry, and four secondary vortex* circulation are set up. Cheng et al. (1977) in their experimental work on curved rectangular channels also observed the formation of four secondary vortices.

* Extensive studies are being undertaken to determine the effect of the shape of the outer wall on the flow field.

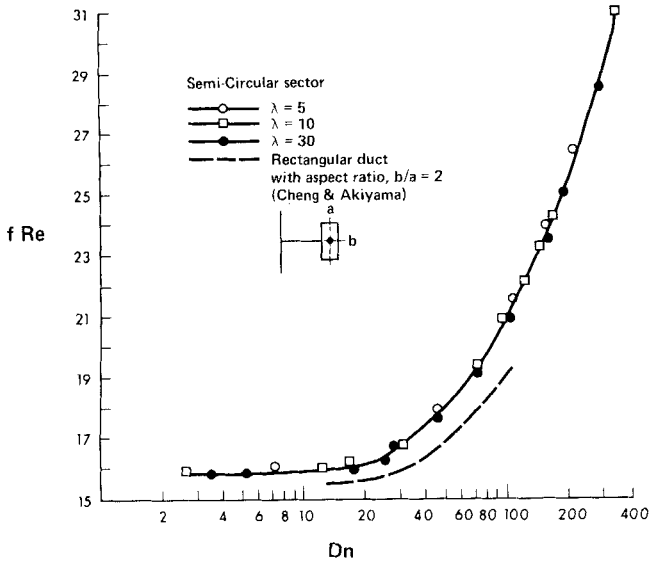

Fig. 5. Variation of *f Re* with Dean number.

It is probable that the shape of the outer wall influences such a shift of location of the maximum velocity (Smith, 1976) and governs the formation of the four secondary vortices. Also shown in Figure 3 are axial velocity profiles corresponding to $\lambda = 30$ and 5, but with the same Dean number. Both profiles are quite similar, and this leads to the possibility of characterizing the flow by Dean number alone.

From the point of heat transfer enhancement, the secondary flow in such tubes is important. Contours of normalized secondary stream function are shown in Figure 4 for low and high Dean numbers. As Dean number is increased, the strength of the secondary flow increases, and the location of the center of circulation shifts towards the two corners of the sector. As the strength of the secondary flow increases, one would expect higher values for friction factor, but this is accompanied by an increase in heat transfer coefficient. The variation of friction factor with Dean number is shown in Figure 5 for $\lambda = 5$, 10, and 30. For this range of curvature values, $f\ Re$ is well represented by Dean number alone and does not depend on individual values of Re and λ. For the case of circular helical tubes, Austin and Seader (1973) and Tarbell and Samuels (1973) found that $f\ Re$ depends on λ in addition to Dn. Results for a rectangular curved tube having an aspect ratio of 2 are compared with the present results. Although for $\lambda \to \infty$ (or $Dn \to 0$) $f\ Re$ for such a rectangular duct is 15.517, which is close to the value of 15.79 for a semicircular sector, deviations occur at higher values of Dn. This is in spite of the fact that equivalent diameter is used as the characteristic length. This points out that equivalent diameter does not completely account for the difference in the geometries. In other words, $f\ Re$ is strongly dependent on the geometry and cannot be correlated by the equivalent diameter alone.

It has already been shown that Dean number can uniquely be used to characterize the normalized axial velocity (Figure 3) and $f\ Re$ (Figure 5). However, Dean number is an implicit value that can be calculated only after a solution of the flow field is obtained. The fundamental parameters are λ and Q. These two parameters explicitly appear in the momentum equations, and consequently they govern the flow field. For the geometry considered in this study, it was found that

$$Q/\lambda^{1.5} = -10.5\, Dn^{1.18}, \quad Dn > 10$$

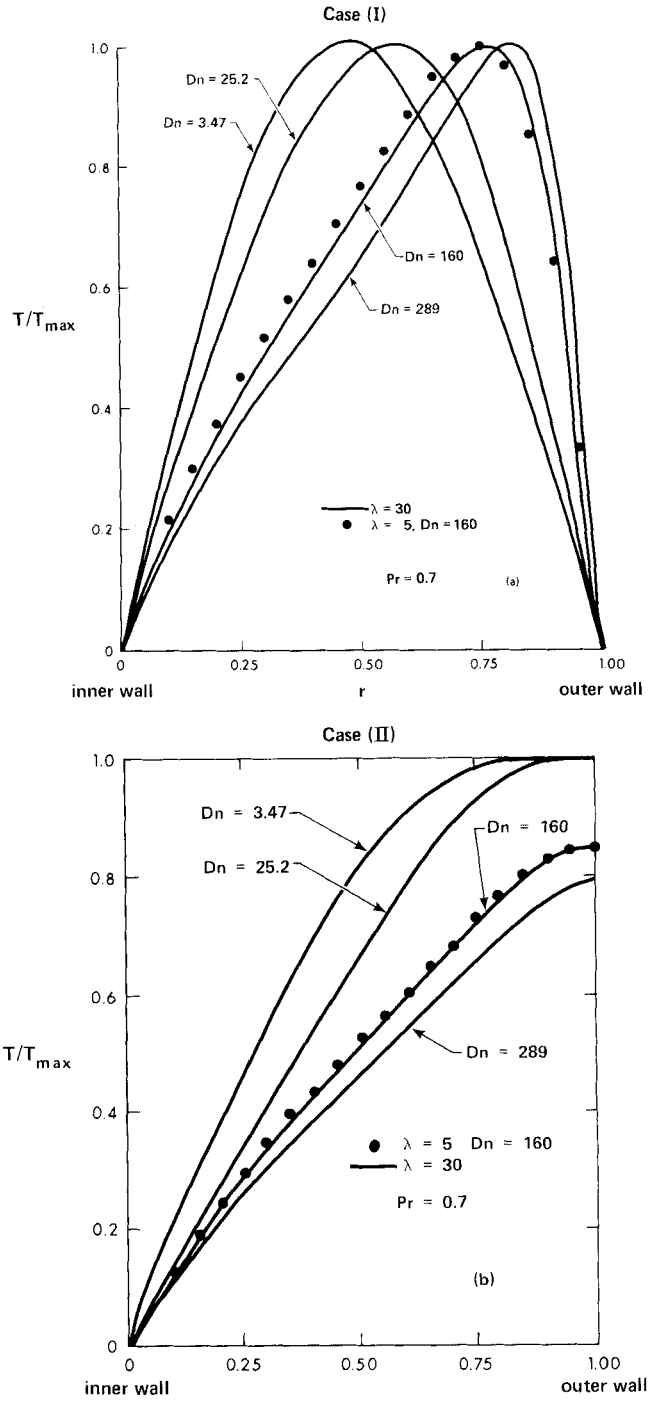

Fig. 6. Radial variation of normalized dimensionless temperature at $\theta = \pi/2$ for $Pr = 0.7$.

The above equation indicates that Dean number is uniquely determined by $Q/\lambda^{1.5}$. Indeed, this single parameter $Q/\lambda^{1.5}$ has been used for the case of $\lambda >> 1$ to characterize the flow in helical circular tubes (McConaloque and Srivastava, 1968; Collins and Dennis, 1975, 1976).

Heat Transfer

The normalized temperature profile for the first set of thermal boundary conditions (case 1) is quite similar to the normalized axial velocity profile. Figure 6*a* shows the normalized temperature profile along r at $\theta = \pi/2$ for various Dn at $Pr = 0.7$ and $\lambda = 30$. Compare this with the axial velocity profile shown in Figure 3. As with the axial velocity profile, decreasing λ to 5 at the same

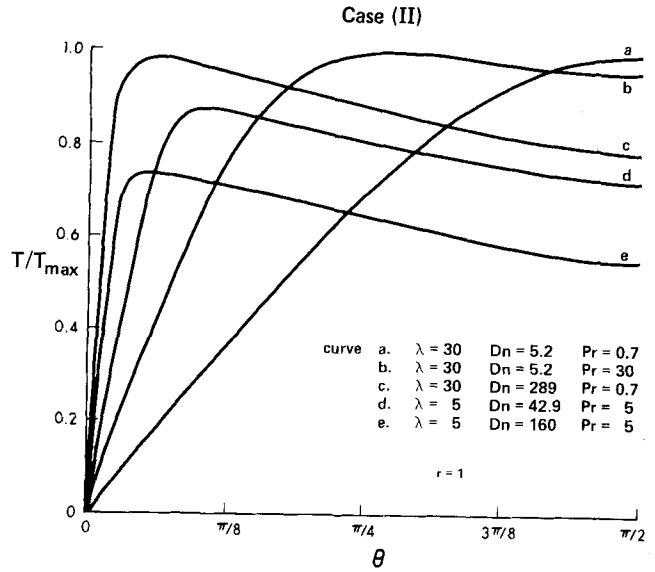

Fig. 7. Angular variation of normalized dimensionless temperature at the outer wall, $r = 1$.

Dn (shown as full circles in Figure 6*a*) gives a profile which is close to the case for $\lambda = 30$. Consequently, *Dn* appears to account quite well for curvature for heat transfer. This is also true for the second set of thermal boundary conditions, as is shown in Figure 6*b*. This observation is brought out more clearly in the plots of the average Nusselt number, shown in Figures 9*a* and 9*b*.

The thermal boundary conditions have a significant effect on the temperature field. This confirms similar observations made earlier by Kalb and Seader (1974) for a different geometry. Compare the temperature profiles for the two cases in Figures 6*a* and *b*. For case 1, the maximum temperature T_{max} occurs along $\theta = \pi/2$, and this location shifts towards the outer wall as *Dn* increases, resembling very closely the axial velocity profile. However, for case 2, as is shown in Figures 6*b*, 7, and 8, T_{max} does not occur along $\theta = \pi/2$ for all *Dn* values. For low *Pr* and *Dn*, the global T_{max} occurs at $r = 1$ and $\theta = \pi/2$. But as *Dn* (or *Pr*) increases, the location of T_{max} shifts along $r = 1$ into the region $\pi/2 > \theta > 0$. Further increase in *Dn* or *Pr* causes the maximum temperature to shift into the region $1 > r > 0$. Increasing *Pr* at a fixed *Dn* and increasing *Dn* at a fixed *Pr* have a similar effect on the convective heat transfer, and the corresponding temperature profiles are expected to show similar qualitative changes.

Figures 9*a* and 9*b* show the variation of the average Nusselt number $\overline{Nu}$ with Dean number for the two heat transfer cases. At low Dean number, the curves for the various values of *Pr* approach the asymptotic Nusselt number value for the case of a straight semicircular duct, and $\overline{Nu}$ becomes independent of Prandtl number. At higher values of *Dn*, the $\overline{Nu}$ vs. *Dn* curves exhibit asymptotic behavior.

Variation of the average Nusselt number with Dean number for the case of a rectangular curved duct with an aspect ratio of 2 is shown in Figure 9*a*. For high *Dn* values, $\overline{Nu}$ vs. *Dn* curve falls below that for a curved semicircular duct. As for the $f\,Re$ variation, the equivalent diameter does not seem to completely account for different geometries.

Akiyama and Cheng (1971) suggested that Nusselt number could be correlated using $Dn\sqrt{Pr}$. For the heat transfer case (1), this work substantiates the findings of

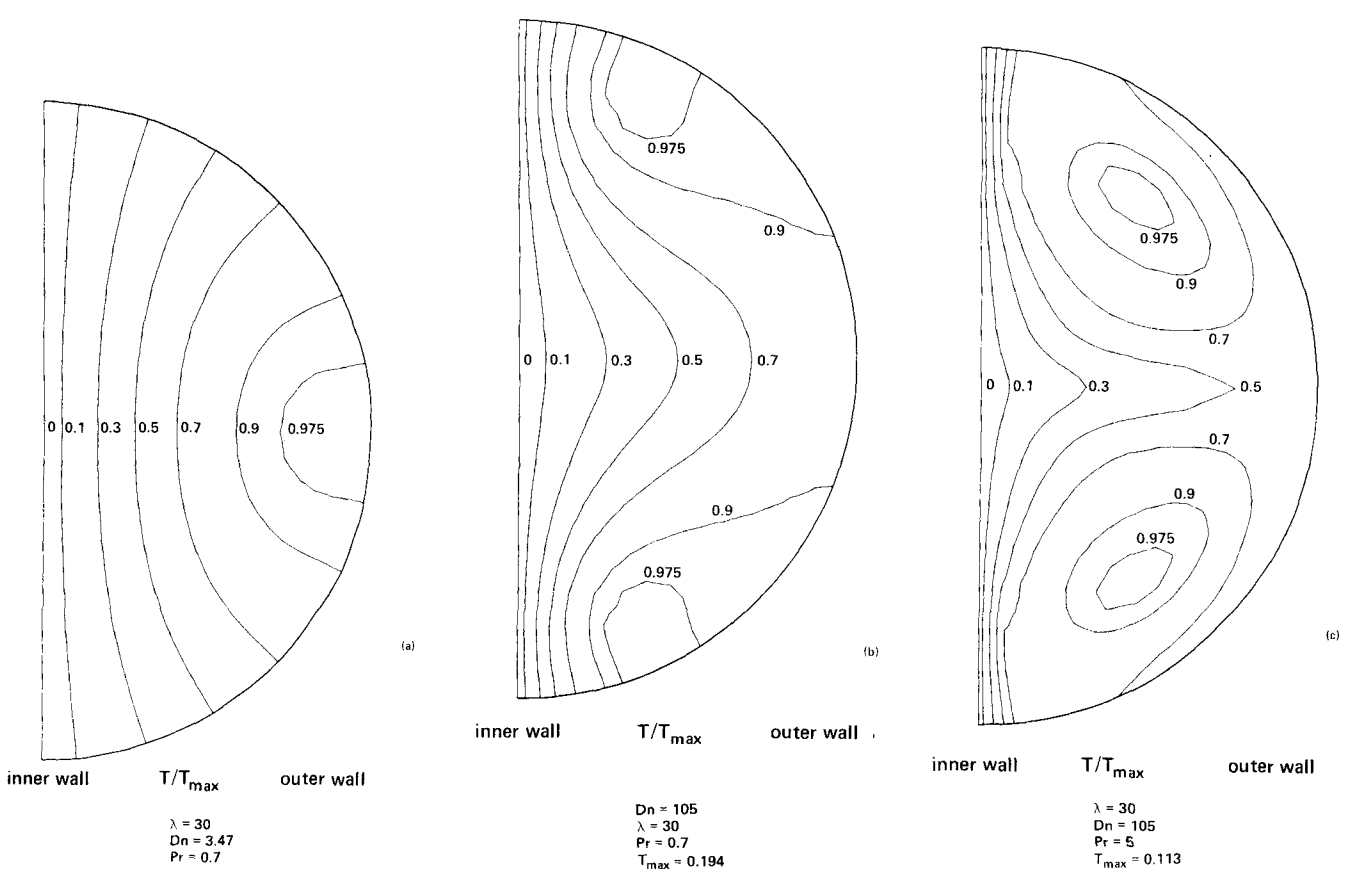

Fig. 8. Contours of normalized dimensionless temperature for case 2.

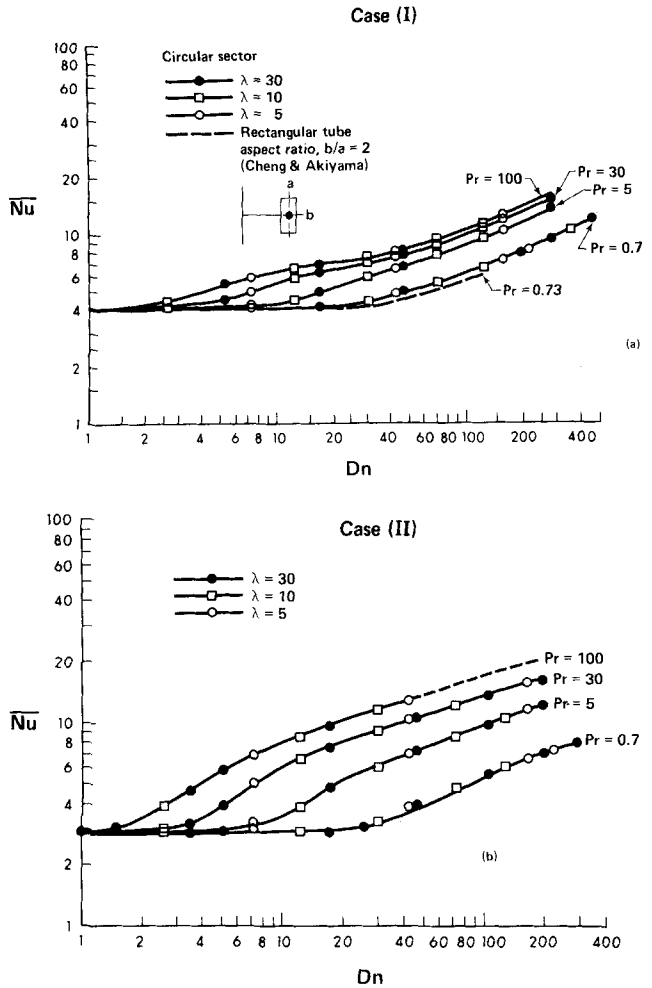

Fig. 9. Variation of average Nusselt number with Dean number.

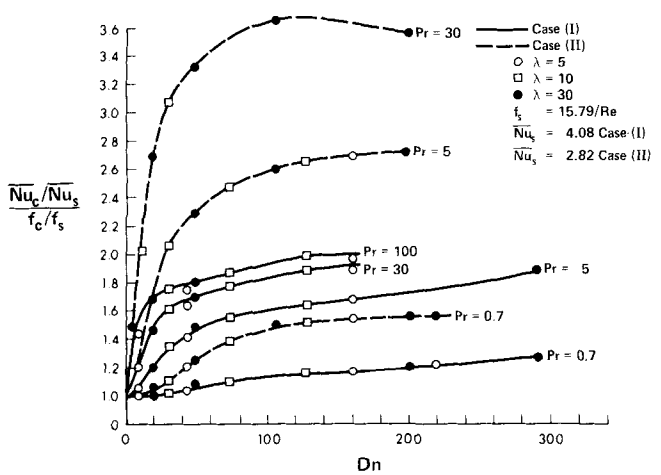

Fig. 10. Enhancement factors for helical semicircular ducts.

Kalb and Seader in that this type of correlation holds true only for a $Dn\sqrt{Pr}$ less than 100. Moreover, for all range of Nu values, the $Dn\sqrt{Pr}$ group was not found useful in correlating the average Nusselt number for case (2).

The fractional increase in heat or mass transfer coefficient relative to the fractional increase in friction factor for curved semicircular duct is shown in Figure 10. In all cases considered, the enhancement factor was higher than unity, and it increases with Dean and Prandtl numbers. The magnitude of the enhancement factors for the case of circular helical tubes was found to be similar to those found here (Kalb and Seader, 1972, 1974). This suggests that the only advantage of using semicircular tubes is in the increase of contact area between the helical tube and the heat transfer surface and in the reduction of the total space requirement for the helical coils.

It should be noted that the present analysis is for the case of a zero pitch coil, that is to say for coils that are very tightly wound. For a large pitch coil, the heat transfer enhancement is expected to be lower than the values presented here.

ACKNOWLEDGMENT

The authors wish to thank the Natural Sciences and Engineering Research Council of Canada and the University of Alberta for financial support.

NOTATION

A_h	=	heat transfer area per unit ϕ, dimensionless
A_w	=	wetted area per unit ϕ, dimensionless
A_x	=	cross-sectional flow area, dimensionless
C_p	=	specific heat of fluid
De	=	equivalent diameter $(4V_w/A_w)$, dimensionless
Dn	=	Dean number $= Re/\sqrt{\lambda}$
f	=	fanning friction factor
h	=	local heat transfer coefficient
h	=	average heat transfer coefficient
$\overline{H}$	=	$\lambda + r\sin\theta$, dimensionless
k	=	thermal conductivity
n	=	coordinate normal to heat transfer surface
$\overline{Nu}$	=	average Nusselt number
p'	=	pressure
Pr	=	Prandtl number
$\overline{q}$	=	heat transfer rate per unit transfer area of coil
Q	=	dimensionless pressure drop $= \partial p'/\partial\phi\ R^2/\nu\mu$
r	=	radial coordinate, Figure 1*a*
R	=	radius of semicircular sector
Rc	=	radius of curvature of coil
Re	=	Reynolds number based on equivalent diameter
T	=	temperature of fluid, dimensionless
T'_b	=	mixing up temperature
T'_w	=	wall temperature
v_i	=	velocity component in i direction, $i = r, \theta, \phi$, dimensionless
$\overline{v_\phi}$	=	mean axial velocity, dimensionless

Greek Letters

Δr	=	grid size in radial direction
$\Delta\theta$	=	grid size in angular direction
θ	=	angular coordinate, Figure 1*a*
λ	=	dimensionless radius of curvature, Rc/R
μ	=	fluid viscosity
ν	=	kinematic viscosity
ρ	=	fluid density
τ	=	dimensionless shear stress
ϕ	=	axial coordinate, Figure 1*a*
ω	=	vorticity, dimensionless
ψ	=	stream function, dimensionless

Subscripts

b	=	bulk average value
c	=	curved tube
max	=	global maximum value
r	=	radial direction
s	=	straight tube
w	=	at the wall

θ = angular direction
ϕ = axial direction
$'$ = dimensional quantity

LITERATURE CITED

Akiyama, M., and K. C. Cheng, "Boundary Vorticity Method for Laminar Forced Convection Heat Transfer in Curved Pipes," *Int. J. Heat Mass Transfer*, **14**, 1659 (1971).

Austin, L. R., and J. D. Seader, "Fully Developed Viscous Flow in Coiled Circular Pipes," *AIChE J.*, **19**, 85 (1973).

Cheng, K. C., J. Nakayama, and M. Akiyama, "Effect of Finite and Infinite Aspect Ratios on Flow Patterns in Curved Rectangular Channels," Proceedings of the International Symposium on Flow Visualization, Tokyo, Japan (Oct., 1977).

Cheng, K. C., and C. J. Hwang, "Numerical Solution for Combined Free and Forced Laminar Convection in Horizontal Rectangular Channels," *J. Heat Transfer*, **91**, 59 (1969).

Cheng, K. C., and M. Akiyama, "Laminar Forced Convection Heat Transfer in Curved Rectangular Channels," *Int. J. Heat Mass Transfer*, **13**, 471 (1970).

Collins, W. M., and S. C. R. Dennis, "The Steady Motion of a Viscous Fluid in a Curved Tube," *Q.J. Mech. Appl. Math.*, **18**, Pt 2, 133 (1975).

———, "Steady Flow in a Curved Tube of Triangular Cross Section," *Proc. Royal Soc.*, **A352**, 189 (1976).

Cuming, H. G., "The Secondary Flow in Curved Pipes," Aeronautical Research Council Reports and Memoranda, #2880 (1952).

Dean, W. R., "Notes on the Motion of Fluid in a Curved Pipe," *Phil. Mag.*, **4**, 208 (1927).

Eckert, E. R. G., et al., "Local Laminar Heat Transfer in Wedge-Shaped Passages," *Trans. ASME*, **80**, 1433 (1958).

Eustice, J., "Flow of Water in Curved Pipes," *Proc. Royal. Soc.*, **A84**, 107 (1910).

———, "Experiments of Stream-Line Motion in Curved Pipes," *ibid.*, **A85**, 119 (1911).

Joseph, B., et al., "Numerical Treatment of Laminar Flow in Helically Coiled Tubes of Square Cross-Section," *AIChE J.*, **21**, 965 (1975).

Kalb, C. E., and J. D. Seader, "Heat and Mass Transfer Phenomena for Viscous Flow in Curved Circular Tubes," *Int. J. Heat Mass Transfer*, **15**, 801 (1972).

———, "Fully Developed Viscous-Flow Heat Transfer in Curved Circular Tubes with Uniform Wall Temperature," *AIChE J.*, **20**, 340 (1974).

Masliyah, J. H., and K. Nandakumar, "Fluid Flow and Heat Transfer in Internally Finned Helical Coils," *The Can. J. Chem. Eng.*, **55**, 27 (1977).

McConalogue, D. J., and R. S. Srivastava, "Motion of Fluid in a Curved Tube," *Proc. Royal Soc.*, **A307**, 37 (1968).

Mori, Y., and Y. Uchida, "Study on Forced Convective Heat Transfer in Curved Square Channel," (1st report Theory of Laminar Region), *Trans. Japan Soc. Mech. Engrs.*, **33**, 1836 (1967).

Rohsenow, W. M., and H. Y. Choi, *Heat Mass and Momentum Transfer*, Prentice-Hall, Englewood Cliffs, N.J. (1961).

Shah, R. K., and A. L. London, "Laminar Flow Forced Convection Heat Transfer and Flow Friction in Straight and Curved Ducts," Tech. Report No. 75, Dept. of Mech. Eng., Stanford University, Stanford, Calif. (1971).

Smith, F. T., "Steady Motion Within a Curved Pipe," *Proc. Royal Soc.*, **A347**, 345 (1976).

Sparrow, E. M., and A. Heji-Sheihk, "Laminar Heat Transfer and Pressure Drop in Isoceles Triangular, Right-Triangular and Circular Sector Ducts," *J. Heat Transfer*, **87C**, 426 (1965).

Srinivasan, P. S., et al., "Pressure Drop and Heat Transfer in Coils," *Chem. Engr.*, **218**, 113 (1968).

Tarbell, J. M., and M. R. Samuels, "Momentum and Heat Transfer in Helical Coils," *Chem. Eng. J.*, **5**, 117 (1973).

Taylor, G. I., "The Criterion for Turbulence in Curved Pipes," *Proc. Royal Soc.*, **A124**, 243 (1929).

Topakoglu, H. C., "Steady Laminar Flows of an Incompressible Viscous Fluid in Curved Pipes," *J. Math. Mech.*, **16**, 1321 (1967).

Truesdell, L. C., Jr., and R. J. Adler, "Numerical Treatment of Fully Developed Laminar Flow in Helically Coiled Tubes," *AIChE J.*, **16**, 1010 (1970).

Weissman, M. H., and L. F. Mockros, "Gas Transfer to Blood Flowing in Coiled Tubes," *A.S.C.E. Proc. Eng. Mech. Div. J.*, **94**, 857 (1968).

Wilkes, M. V., *A Short Introduction to Numerical Analysis*, p. 74, Cambridge Univ. Press, England (1966).

Manuscript received June 9, 1978; revision received December 7, and accepted January 11, 1979.

A Study of Disaggregation Effects in Sedimentation

P. M. ADLER

L.B.H.P. (tour 33/34; 2ème ét.)
Université Paris VII
2, Place Jussieu
75221—Paris Cedex 05

Aggregates are considered as a porous medium. Stresses within the porous solid matrix are calculated when the particle deformation is ignored. The maximum size of the aggregates is derived from a yield condition, and the settling velocity is deduced. The influence of the mechanical properties and concentration of the aggregates are detailed and discussed.

SCOPE

Sedimentation plays an important role in many chemical engineering processes and is also important in medicine (where erythrocyte sedimentation has become a standard clinical test) and in meteorology. The aggregation of particles or formation of clusters has long been recognized as an important factor when dealing with particles suspended in liquids.

Hence, the main objectives of this work are to gain insight into the mechanisms involved and to predict the maximum size of an aggregate when it settles. The aggregate is broken by forces generated by the motion; the larger the aggregate, the larger its settling velocity and thus the larger are these rupture forces. Consequently, we need a model to describe the flow within the aggregate and a model to relate the breakup of the aggregate to the flow field.

More precisely, the flow inside the aggregate, considered as a porous medium, is described by a Brinkman equation. The free cell model is then used to predict the velocity and pressure fields inside and outside the porous medium. Stresses within the porous solid matrix are gen-